Contribution of synthetic lethality to cancer risk, onset age, and tumor suppressor specificity across human tissues

Kuoyuan Cheng[1,2,*], Nishanth Ulhas Nair[1,*], Joo Sang Lee[1,3], and Eytan Ruppin[1,2,#]

1. Cancer Data Science Laboratory (CDSL), National Cancer Institute (NCI), National Institutes of Health (NIH), Bethesda, MD, USA.
2. Center for Bioinformatics and Computational Biology, University of Maryland, College Park, MD, USA.
3. Samsung Medical Center, Sungkyunkwan University School of Medicine, Suwon 16419, Republic of Korea.
* equally contributing co-first authors.
# corresponding author, email: eytan.ruppin@nih.gov

Abstract

Various characteristics of cancers exhibit tissue-specificity, including lifetime cancer risk, onset age and cancer driver genes. The large variation in cancer risk across human tissues was found to strongly correlate with the number of stem cell divisions and abnormal DNA methylation levels occurring in them. Here we study the role of synthetic lethality, an important determinant of cancer fitness, in cancer risk. We find that normal tissues with more down-regulated cancer synthetic lethal (cSL) gene pairs have lower cancer risk and develop cancer at later ages. These associations arise mainly from functional cSL interactions and not from individual gene effects. Further, we show that the tissue-specificity of several tumor suppressor genes can be accounted for by their SL partners' expression. Overall, our findings uncover the role of synthetic lethality as an important independent factor explaining cancer risk, onset age, and the context-specificity of tumor suppressors across human tissues.

Significance: These results point to cancer synthetic lethality (cSL) as an additional independent factor associated with tissue variation in human cancer risk, onset age, and tumor suppressor specificity. Beyond its value in identifying and targeting cancer vulnerabilities, this is the first time that cSL is shown to mediate cancer development.

Introduction

Cancers of different human tissues have hugely different molecular, phenotypic and epidemiological characteristics, known as the tissue-specificity in cancer. Various aspects of this intriguing phenomenon include the variation in lifetime cancer risk, cancer onset age and the genes driving the cancer across tissue types. The variation in lifetime cancer risk is known to span several orders of magnitude (1,2). Such variation cannot be fully explained by the difference in exposure to carcinogens or hereditary factors, but has been shown to strongly correlate with differences in the number of lifetime stem cell divisions (NSCD) estimated across tissues (2,3). Although their original interpretation in Tomasetti and Vogelstein, 2015 (2) was controversial, these findings are consistent with the notion that tissue stem cell divisions can propagate mutations caused either by environmental carcinogens or random replication error (4). Additionally, the importance of epigenetic factors in carcinogenesis has long been recognized (5), and Klutstein *et al.* have recently reported that the levels of abnormal CpG island DNA methylation (LADM) across tissues is highly correlated with their cancer risk (6). Although both global (e.g. smoking and obesity) and various cancer type-specific (e.g. HCV infection for liver cancer) risk factors have been well-known (7), no factors other than NSCD and LADM have been reported to explain the *across-tissue variance* in lifetime cancer risk.

Besides lifetime cancer risk, cancer onset age, as measured by the median age at diagnosis, also varies among adult cancers (1). Although most cancers typically manifest later in life (over 40 years old (1,8)), some such as testicular cancer often have earlier onset (1). Many tumor suppressor genes and oncogenes are also tissue specific (9–11). For example, mutations in the tumor suppressor gene BRCA1 are predominantly known to drive the development of breast and ovarian cancer, but rarely other cancer types (12). In general, factors explaining the overall tissue-specificity in cancer could be tissue-intrinsic (10,13), and their elucidation can further advance our understanding of the forces driving carcinogenesis.

Synthetic lethality/sickness (SL) is a well-known type of genetic interaction, conceptualized as cell death or reduced cell fitness that occurs under the combined inactivation of two genes, but not under the inactivation of either gene alone. The phenomenon of SL interactions was first recorded in *Drosophila* (14) and then in *Saccharomyces cerevisiae* (15). Targeting cancer SLs (cSLs) has been recognized as a highly valuable approach for cancer treatment (16–19). The role of cSL in determining cancer cell fitness has led us to investigate whether it plays an additional role even before cancers manifest, i.e. during carcinogenesis. Here we show that cSL load in normal tissues can explain the variation in cancer risk and cancer onset age across human tissues, as well as the tissue-specificity of numerous tumor suppressor genes. Taken together, our findings support the importance of synthetic lethality in impeding tumorigenesis across human tissues.

Results

Computing cSL load in normal tissue and cancer samples

We use a recently published reference set of cSLs that are common to many cancer types, which have been identified from both *in vitro* and the TCGA cancer patient data via the ISLE method (20,21) (Table S1a). We assessed the co-inactivation status of the genes in each cSL gene pair in large-scale collections of cancer and normal tissues from the TCGA (22) and GTEx (23) datasets, respectively. Specifically, for each sample, we computed the fraction of all the cSLs in our reference set that have *both genes lowly expressed* in that sample (Methods). We term this fraction of lowly expressed cSL pairs its cSL load. The cSL load of a cancer sample is a proxy measure of the cancer cell fitness, since by definition the co-inactivation of cSL gene pairs can reduce cell fitness. We proceed to investigate the association between cSL load of normal tissues and cancer risk, as outlined in **Fig. 1a**.

cSL load is negatively correlated with cancer proliferation and is lower in cancer vs the corresponding normal tissues

We first set out to verify that the ISLE-inferred cSL gene pairs indeed confer pan-cancer lethal effects. We computed the tumor proliferation index (24) for each of the

TCGA cancer samples and correlated that with their cSL load (Methods). We find a significant overall dominance of negative correlation between cSL load and tumor proliferation across all cancer types (binomial test on the direction of correlation P = 4.63e-7, **Fig. 1b**, individual examples with FDR < 0.05 are provided in **Fig. 1c**). Since ISLE identifies cSLs by mining the TCGA data, we further ran the ISLE algorithm in a cross-validation mode using only part of the TCGA samples to identify the cSLs, then we confirmed the above correlation pattern with the held-out samples (Fig. S1, Supp. Note). We additionally performed several random control tests to demonstrate that the effect is specific to cSL (Supp. Note). cSL load also negatively correlates with measured growth rates in cancer cell lines (25) (Spearman's ρ = -0.285, P = 0.013, **Fig. 1d**), confirming the notion that inactivation of cSL gene pairs have lethal/sickness effects on cancer cells. Thus, high cSL load is detrimental to cancer cell fitness, and hence should be overcome as cells become cancerous and highly proliferating.

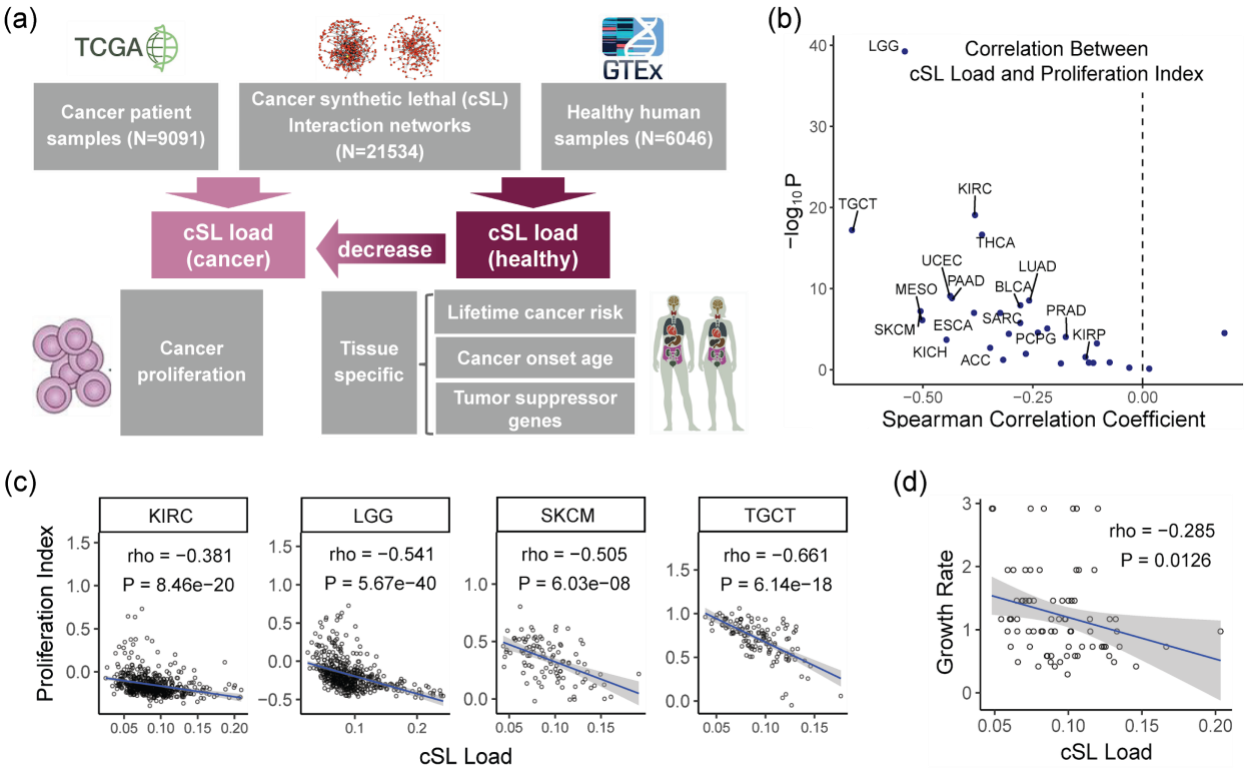

Figure 1. ***(a)*** *An overview of the analyses performed to study the relations between cSL load and different cancer-related phenotypes.* ***(b)*** *A volcano plot displaying the*

correlations between cSL load and the tumor proliferation index for each TCGA cancer type. The Spearman's correlation coefficient is denoted on the X-axis and its significance (negative log of P value) on the Y-axis. In the majority of cancer types cSL load negatively correlates with proliferation index (binomial test P = 4.63e-7). Standard TCGA cancer type abbreviations are used in the label. Examples of four cancer types are given in ***(c)****, all the examples have FDR < 0.05.* ***(d)*** *Correlation between cSL load and experimentally measured growth rates in 76 breast cancer cell lines* (25)*.*

Next, we turned to compute the cSL loads of the GTEx normal tissue samples and compared them to those of the TCGA cancers of matching types. In the majority of the cases we observe that, indeed, the cSL load decreases from normal to cancer (binomial test on the direction of effect P = 6.61e-3, **Fig. 2a**, individual examples with FDR < 0.05 in **Fig. 2b**). This suggests that, as normal cells undergo malignant transformation they need to reactivate at least some of the down-regulated cSL genes for the emerging cancer cells to survive. This observation also holds when we identify the cSLs by applying ISLE only to a subset of the TCGA samples and then perform the comparison between the matching tumor and normal tissues on the held-out samples (Fig. S2, Supp. Note; additional randomized control tests were also performed). Furthermore, we find that the cSL load decreases progressively as cancers develop from normal tissues through the multiple stages of premalignant lesions using a recently published lung cancer dataset (26) (**Fig. 2c**, normal vs cancer Wilcoxon rank-sum test P = 4.47e-5, ordinal logistic regression P = 5.89e-7 with negative coefficient -28.7; Methods). These findings thus give rise to the hypothesis that high cSL load in the normal tissues can act as a barrier to cancer development.

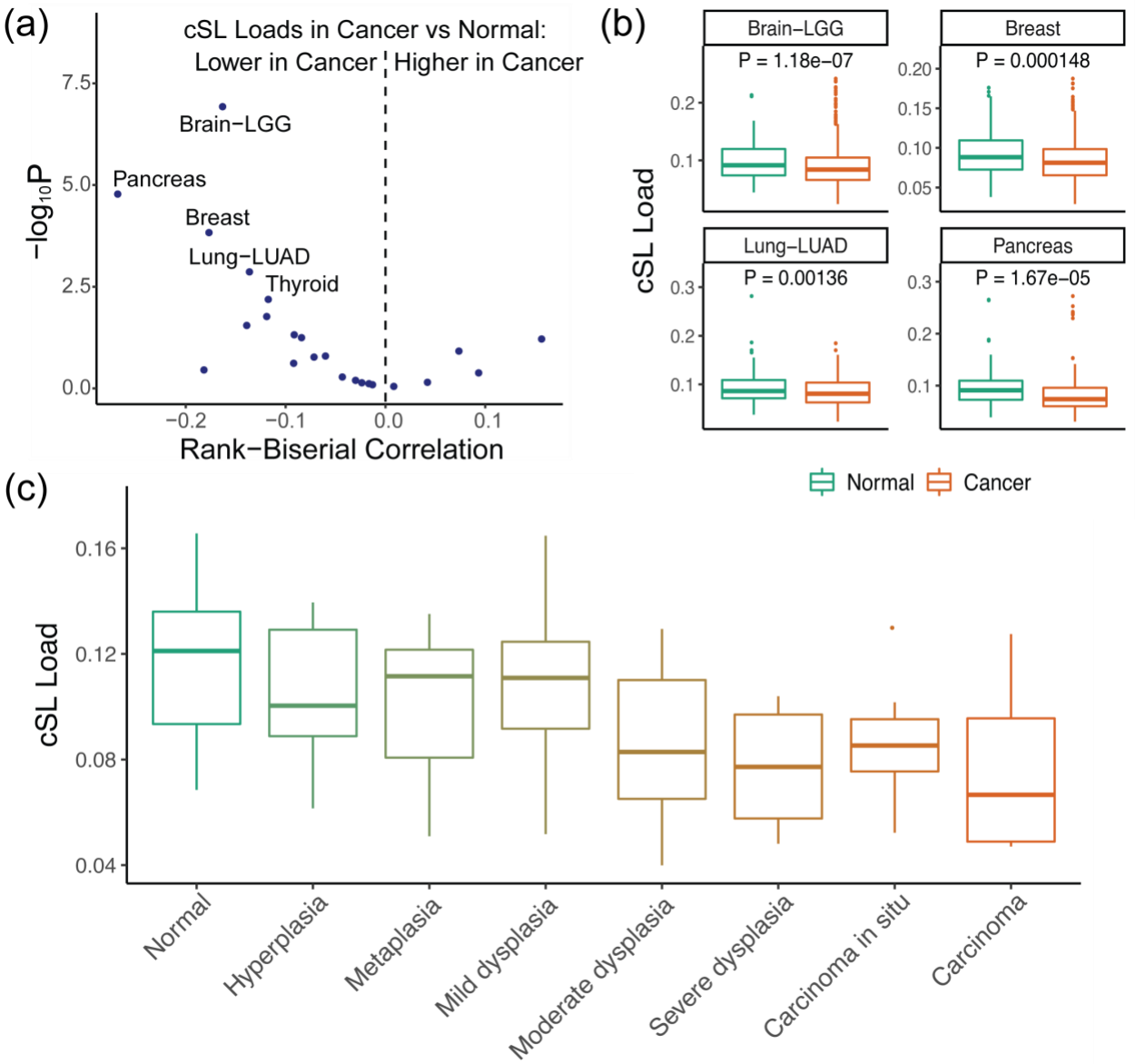

Figure 2. ***(a)*** *A Volcano plot summarizing the comparison of cSL loads in GTEx normal tissues vs matched TCGA cancer types. cSL load differences were analyzed using Wilcoxon rank-sum tests (whose significance value is presented on the Y-axis) with effect size represented by rank-biserial correlation (X-axis). A negative rank-biserial correlation means that the cSL load is lower in cancer vs the corresponding type of normal tissue, and vice versa). There is an overall decrease in cSL load in cancers compared to the matched normal tissues observed for most of the cases (binomial test P = 6.61e-3). GTEx tissue names (and the matched TCGA cancer type abbreviation in cases where multiple cancer types can be matched to the same tissue type) are used to label the data points.*

*Four example tissues are shown in **(b)**, all the examples have FDR < 0.05. **(c)** The cSL load in samples of different stages of pre-malignant lesions in the lung (including normal tissue and lung squamous cell carcinoma) (26). The cSL load shows an overall decreasing trend from normal through different pre-cancer stages to cancer (one-sided Wilcoxon rank-sum test of normal vs cancer P = 4.47e-5; ordinal logistic regression has negative coefficient -28.7, P = 5.89e-7).*

Tissue cSL load in normal tissues is inversely correlated with their lifetime cancer risk

Different normal tissues have varied cSL load levels due to their specific expression profiles. Based on the findings presented in the previous section, we hypothesized that normal tissues with higher cSL loads should have lower cancer risk, as transforming cancerous cells in these tissues will face higher cSL-mediated vulnerability and lethality. To test this, we computed the tissue cSL load (TCL), the median value of cSL loads in the samples of a tissue (Methods, Table S2a). Notably, we find a strong negative correlation between the TCL (computed from older-aged GTEx samples, age ≥ 50 years) and lifetime cancer risk across normal tissues (Spearman's ρ = -0.664, P = 1.59e-4, **Fig. 3a**, Table S2a). This correlation is robust, as comparable results are obtained when this analysis is carried out in various ways (e.g. different cutoffs for low expression of genes, different cSL network sizes, different cancer type-normal tissue mappings, etc., Fig. S3, Supp. Note). Notably, the cSL load varies with age due to age-related gene expression changes, and the correlation with lifetime cancer risk is not found when the TCL is computed on samples from the young population (20 ≤ age < 50 years, Spearman's ρ = -0.0251, P = 0.901, Fig. S4a); this is consistent with the observation that lifetime cancer risk is mostly contributed by cancers occurring in older populations (1). Importantly, we still see a marked negative correlation between TCL and lifetime risk when analyzing samples from all age groups together (Spearman's ρ = -0.49, P = 0.01, Fig. S4b). Repeating these analyses using different control gene-pairs, including (i) random gene pairs; (ii) shuffled cSL gene pairs; and (iii) degree-preserving randomized cSL network (same size as the actual cSL network, Supp. Note) results in significantly

weaker correlations (empirical P < 0.001, Fig. S5a-c, Supp. Note), confirming that the associations found with cancer risk results from a cSL-specific effect.

The association between cSL and cancer risk arises from the genetic interaction rather than single-gene effects

While the randomized cSL networks used in the control tests described above provide significantly weaker correlations with cancer risk than those observed with cSLs, many of these correlations are still significant by themselves (Fig. S5b,c). This suggests that there may be a possible association between the expression of single genes in the cSL network (*cSL genes*) and cancer risk. To investigate this, we computed the *tissue cSL single-gene load* (*SGL*, the fraction of lowly expressed cSL genes) for each tissue (Methods). Indeed, we do find a significant negative correlation between tissue SGL levels and cancer risk (Spearman's ρ = -0.49, P = 0.01, Fig. S5d, Supp. Note). This correlation vanishes when we used random sets of single genes (Fig. S5f). However, after controlling for the single-gene effect, the partial correlation between tissue cSL load and cancer risk is still highly significant (Spearman's rho = -0.69, P = 6.10e-5, Fig. S5g), pointing to the dominant role of the SL genetic interaction effect (Supp. Note).

Tissue cSL load adds to the number of tissue stem cell division and abnormal DNA methylation level in predicting lifetime cancer risk across tissues

We next compared the predictive power of TCL to those obtained with the previously reported measures of NSCD (2,3) and LADM (6), using the set of GTEx tissue types investigated here (Methods). We first confirmed the strong correlations of NSCD and LADM with tissue lifetime cancer risk in our specific dataset (Spearman's ρ = 0.72 and 0.74, P = 2.6e-5 and 1.3e-4, respectively, Fig. S6). These correlations are stronger than the one we reported above between TCL and cancer risk. However, adding TCL to either NSCD or LADM in linear regression models leads to enhanced predictive models of cancer risk compared to those obtained with NSCD or LADM alone (log-likelihood ratio = 2.18 and 2.39, P = 0.037 and 0.029, respectively). Furthermore, adding TCL to each of these factors increases their prediction accuracy under cross-validation (Spearman's ρ's from 0.67 and 0.69 with NSCD and LADM alone to 0.71 and 0.77, respectively, **Fig. 3b,c**).

LADM and NSCD are significantly correlated (Spearman's ρ = 0.66, P = 0.02), while the TCL correlates only in a borderline significant manner with either NSCD (Spearman's ρ = -0.57, P = 0.06) or LADM (Spearman's ρ = -0.52, P = 0.08). Taken together, these observations support the hypothesis that cSL is associated with tissue cancer risk, with a partially independent role from either NSCD or LADM.

cSL pairs whose genes are differentially upregulated in cancer vs normal tissues are more predictive of cancer risk

We have shown that cancers have decreased cSL loads vs normal tissues. That is, many cSL gene pairs are "*released*" from their combined low expression state in the normal tissues as cancer emerges, although some other cSL pairs can still remain co-lowly-expressed ("*retained cSLs*"). We identified these two sets of SLs for each of the 13 GTEx tissues for which matching TCGA data is available (Methods, Table S4). We hypothesized that the released cSLs are those whose co-inactivation is more detrimental to the developing tumors. Indeed, we find that the released cSLs are assigned stronger significance values by ISLE (20) (i.e. are likely to have stronger lethal effect on cancer cells) than the retained cSLs (FDR < 0.05; only one tissue shows the opposite trend; **Fig. 3d**). More importantly, the TCLs computed from the released cSLs correlate much stronger with cancer lifetime risk than those computed from the retained cSLs (Spearman's ρ = -0.593 vs -0.319, **Fig. 3e** left side), testifying that these functionally strong cancer cSLs are truly relevant to carcinogenesis. The released cSLs are enriched for cell cycle, DNA damage response and immune-related genes (FDR < 0.05, Table S5, Methods), which are known to play key roles in tumorigenesis.

Higher tissue cSL load in the younger population is associated with delayed cancer onset

We have thus established that TCL in the older population is inversely correlated with lifetime cancer risk across tissues. We next hypothesized that higher cSL load in a tissue in the young population may impede cancer development and delay cancer onset, which typically occur later (age > 40 years (1)). To test this, we use the median age at cancer diagnosis (1) of a certain tissue as its cancer onset age (Table S3, Methods). We find that the TCL values (for age ≤ 40 years) are indeed markedly correlated with cancer

onset age (Spearman's ρ = 0.502, P = 0.011, **Fig. 3f**). This result is again robust to variations in our methods to compute TCL and cancer onset age (Fig. S7, Table S3, Supp. Note). We note that the cancer onset age is not significantly correlated with lifetime cancer risk (Spearman's ρ = 0.279, P = 0.28).

Similar to our earlier analysis, we see that the TCLs computed from the released cSLs correlate much stronger with onset age than those from the retained or all cSLs (Spearman's ρ = 0.603 vs -0.157, **Fig. 3e** right side, Fig. S8a), and also than those obtained from control tests performed as before (empirical P < 0.001, Fig. S8b-d). As with the case of cancer risk, the observed correlation is dominated by the SL genetic interaction effect rather than the single gene effect (Fig. S8e-g, Supp. Note).

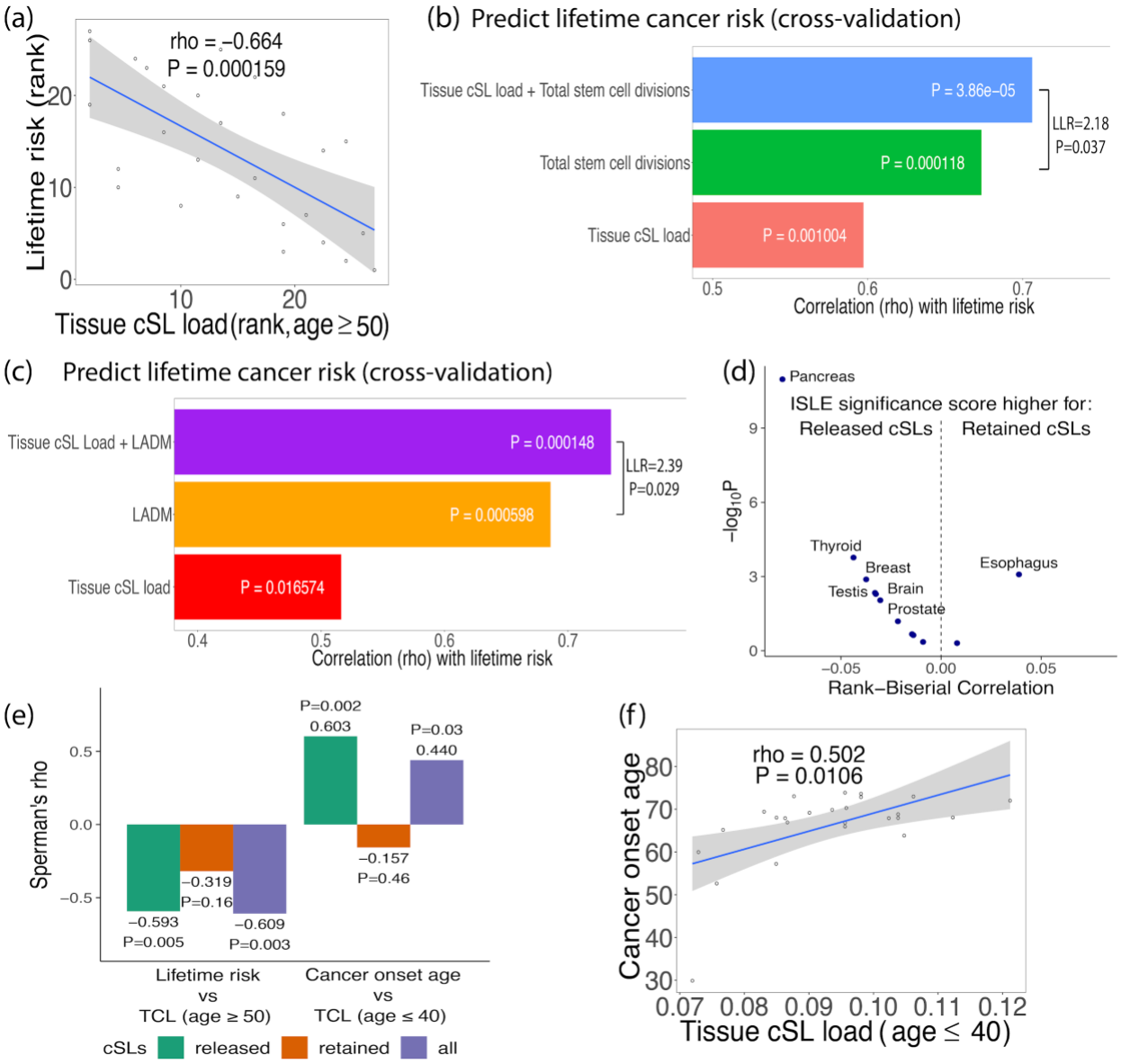

Figure 3. *Scatter plots showing the Spearman's correlations between lifetime cancer risk and:* ***(a)*** *tissue cSL load (TCL) computed for the older population (age ≥ 50 years);* ***(b)*** *Lifetime cancer risks across tissues were predicted using linear models (under cross-validation) containing different sets of explanatory variables, which are: (1) TCL only; (2) the number of stem cell divisions (NCSD) only; and (3) TCL and NSCD (27 data points). The prediction accuracy is measured by the Spearman's ρ (rho), shown by the bar plots. The result of a likelihood ratio test between model (2) and model (3) is also displayed.* ***(c)*** *A similar bar plot as in (b) comparing the predictive models for cancer risk involving the variables: (1) TCL only; (2) the level of abnormal DNA methylation (LADM) only; and (2)*

TCL and LADM combined (21 data points only due to the smaller set of LADM data). A model containing all the three variables does not increase the prediction power (Spearman's ρ = 0.77 under cross-validation) and is not shown. ***(d)*** *A Volcano plot summarizing the comparison of ISLE significance score between the released and retained cSLs in each tissue. ISLE significance score differences were analyzed using Wilcoxon rank-sum tests (whose significance value is presented on the Y-axis) with effect size represented by rank-biserial correlation (X-axis). A negative rank-biserial correlation value means that the released cSLs have higher significance scores than the retained cSLs, and vice versa.* ***(e)*** *TCLs for age ≥ 50 years and 20 ≤ age ≤ 40 years were computed using the released cSLs, the retained cSLs, or all cSLs (Methods), and the TCLs of the older and younger population were correlated with lifetime cancer risk and cancer onset age, respectively. The bar plot shows the Spearman's ρ's and P values of these correlations. This analysis was performed using only the subset of GTEx tissues that can be mapped to TCGA cancer types such that the released or retained cSLs can be determined.* ***(f)*** *Scatter plots showing the Spearman's correlations between cancer onset age and TCL (age ≤ 40 years). Ranked values are used in the figure involving lifetime cancer risk, which spans several orders of magnitude.*

The *activity state of cSL partners of some tumor suppressor genes predicts the specific tissues in which they are known to drive cancer*

Further investigating the role of cSLs in cancer development, we turned to ask whether cSL may also contribute to the tissue/cancer-type specificity of tumor suppressor genes (TSGs) (10,27). Specifically, we reasoned that loss-of-function mutations of a TSG during carcinogenesis will be less frequent in tissues where its *cSL partner genes* are lowly expressed, due to the synthetic lethal effect of such co-inactivation on the emerging cancer cells. To study this hypothesis, we obtained a list of TSGs together with the tissues in which their loss is annotated to have a tumor-driving function from the COSMIC database (11) (Table S6a). We further identified the cSL partner genes of each such TSG using ISLE (20) (Methods, Table S6b). In total, there are 23 TSGs for which we were able to identify more than one cSL partner gene. Consistent with our hypothesis, we find that

in the majority of the cases, the cSL partner genes of TSGs have higher expression levels in the tissues where the TSGs are known drivers compared to the tissues where they are not established drivers (binomial test for the direction of the effect P = 0.023, **Fig. 4a**). We performed proper randomized control tests involving random partner genes of the TSGs and shuffled TSG-tissue type mapping to ensure the specificity of the observed effect (Supp. Note). We identified 10 TSGs whose individual effects are significant (FDR < 0.05) as well as cSL-specific (as shown by the random control test), and all these 10 cases exhibit the expected direction of effect (labelled in **Fig. 4a**, Table S6c; two example TSGs, FAS and BRCA1, are shown in **Fig. 4b**, details in Fig. S9, Methods). These results further consolidate the role of cancer-specific cSLs of normal tissues in cancer risk and development.

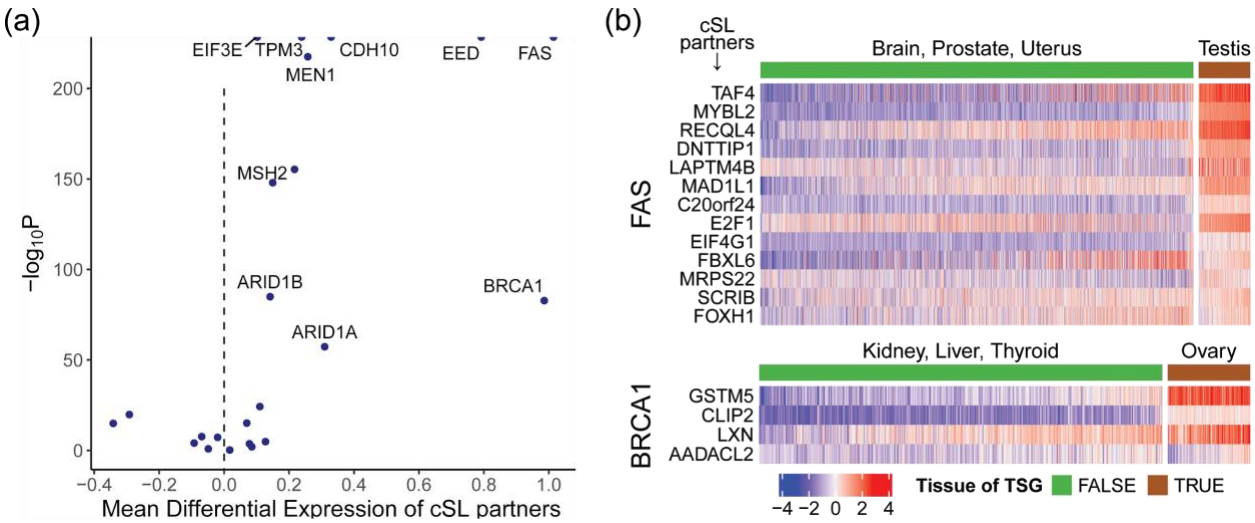

Figure 4. ***(a)*** *For each tissue-specific tumor suppressor (TSG) gene G_i, the expression levels of its cSL partner genes in the tissue type(s) where gene G_i is a TSG were compared to those where gene G_i is not an established TSG, using GTEx normal tissue expression data. The volcano plot summarizes the result of comparison with linear models. Positive linear model coefficients (X-axis) mean that the expression levels of the cSL partner genes are on average higher in the tissue(s) where gene G_i is a TSG. Many cases have near-zero P values and are represented by points (half-dots) on the top border line of the plot. Overall there is a dominant effect of the cSL partner genes of TSGs have*

higher expression levels in the tissues where the TSGs are known drivers (binomial test P = 0.023). All TSGs with FDR < 0.05 that also passed the random control tests are labeled. ***(b)*** *Examples of two well-known TSGs, FAS and BRCA1, are given. The heatmaps display the normalized expression levels of their cSL partner genes (rows) in tissues of where these two genes are known to be TSGs and in tissues where they are not established TSGs (columns), respectively. High and low expression are represented by red and blue, respectively. For clarity, one typical tissue type where the TSG is a known driver (e.g. testis for FAS) and three other tissue types where the TSG is not an established driver (and the least frequently mutated) are shown.*

Discussion

In this work we show that the cSL load in normal tissues is a strong predictor of tissue-specific lifetime cancer risk. Notably, this effect is primarily mediated by the SL genetic interaction and is much stronger than any effects observed on the individual gene level. Consistently, we find that higher cSL load in the normal tissues from young people is associated with later onset of the cancers of that tissue. As far as we know, no other factor has been previously reported to be predictive of cancer onset age across tissues. Finally, we show that the activity status of cSL partners of tumor suppressor genes can explain their tissue-specific inactivation.

Our work is based on the computation of cSL load, which reflects the summed effects of individual cSL gene pairs from the entire cSL network in a given sample. The underlying assumption is that the low expression of each cSL gene pair is synthetic sick (i.e. reducing cell fitness to some extent), and that the effects from different cSL gene pairs are additive, consistent with the ISLE method of cSL identification (20). Indeed, many experimental screening of SL interactions also rely on techniques such as RNA interference that inhibits gene expression rather than completely knocks out a gene (28), and it is evident that most of the resulting SL gene pairs have milder than lethal effects. Accordingly, cancer samples have low (albeit non-zero) cSL load, where the variation in cSL load corresponds to the proliferation rates of cancer cells, as we have shown. Yet

one may wonder why the normal tissues exhibit higher cSL load without a decrease in tissue viability. We think that this is likely because these *cancer* SLs tend to be specifically functional in cancers rather than normal tissues. Indeed, we tested and find that the co-inactivation of cSL gene pairs is under much weaker negative selection in GTEx normal tissues vs matched TCGA cancers (Wilcoxon rank-sum test P = 2.93e-6, Fig. S10a, also shown using cross-validation, Supp. Note). Some of the cSLs do seem to exhibit mild negative selection in the normal tissues, but we note that irrespective of this, cSLs can form a negative force impeding cancer development from normal cells as they have strong lethal effects in cancers.

Obviously, as we are studying the across-tissue association between cSL load and cancer risk, it is essential to focus on cSLs that are common to many cancer types. Therefore, we focused on cSLs identified computationally by ISLE via the analysis of the pan-cancer TCGA patient data (20). In contrast, most experimentally identified cSLs are obtained in specific cancer cell lines and are thus less likely to be pan-cancer (and possibly, less clinically relevant (20)). However, for completeness, we also compiled a set of experimentally identified cSLs from published studies (20,29) (Supp. Note, Table S1b). The corresponding TCL values computed using this set of cSLs also correlates significantly with lifetime cancer risk, although markedly weaker than that obtained from ISLE-derived cSLs (Spearman's ρ = -0.433, P = 0.024, Fig. S11a, control tests and detailed analysis explained in Supp. Note). This corroborates the importance of pan-cancer cSLs and their relevance to cancer risk.

Interestingly, tissue cSL load is not likely a corollary of the number of tissue stem cell divisions (NSCD) and DNA methylation (LADM; the latter was thought to be closely related to NSCD (6)), as cSL load is computed by analyzing bulk tissues, where stem cells occupy only a minor proportion. Accordingly, we confirmed that the proliferation indices computed for the bulk normal tissues do not correlate with lifetime cancer risk across tissues (Spearman's ρ = 0.062, P = 0.77, Fig. S12, Supp. Note). Moreover, we have shown that TCL significantly adds to either NSCD or LADM in predicting lifetime cancer risk, suggesting that cSL load is an independent factor of cancer risk acting via

unique mechanisms. We also further verified that our observed correlations are not confounded by the number of samples from each cancer or tissue type (Fig. S13).

Taken together, our findings demonstrate the contribution of synthetic lethality to cancer risk, onset time, and context-specificity of tumor suppressors across human tissues. Beyond the effect on cancer after it has developed, our work highlights the role of cancer synthetic lethality during the entire course of carcinogenesis. While synthetic lethality has been attracting tremendous attention as a way to identify cancer vulnerabilities and target them, this is the first time that its role in mediating cancer development is uncovered.

Methods

Cancer SL (cSL) interaction networks

The cSL gene pairs computationally identified by the ISLE (identification of clinically relevant synthetic lethality) pipeline was obtained from (20). We used the cSL network identified with FDR < 0.2 for the main text results, containing 21534 cSL gene pairs, which is a reasonable size represents only about 1 cSL partner per gene on average. This also allows us to capture the effects of many weak genetic interactions. Nevertheless, we also used the cSL network with FDR < 0.1 (only 2326 cSLs) to demonstrate the robustness of the results to this parameter (Supp. Note). Each gene pair is assigned a significance score (the “SL-pair score” defined in Lee *et al.* 2018 (20)), that a higher score indicates that there is stronger evidence that the gene pair is SL in cancer. Out of these, we used 20171 cSL gene pairs whose genes are present in the GTEx data (Table S1a). The experimentally identified cSL gene pairs were collected from 18 studies (references in Supp. Note. Obtained from the Supplementary Data 1 of Lee *et al.* 2018 except for those from Horlbeck *et al.* 2018 (29)). Horlbeck *et al.* provided a gene interaction (GI) score for each gene pair in two leukemia cell lines. Gene pairs with GI scores < -1 in either cell line were selected as cSLs. A total of 27975 experimentally identified cSLs were obtained, out of which 27538 have both their genes present in the GTEx data (Table S1b).

GTEx and TCGA data

The V6 release of Genotype-Tissue Expression (GTEx) (23) RNA-seq data (gene-level RPKM values) were obtained from the GTEx Portal (https://gtexportal.org/home/). The associated sample phenotypic data were downloaded from dbGaP (30) (accession number phs000424.vN.pN). To enable the comparison of gene expression between normal and cancer tissues, the RNA-seq data of the Cancer Genome Atlas (TCGA) and GTEx as RSEM values that have been processed together with a consistent pipeline that helps to remove batch effects were downloaded from UCSC Xena (31). The expression data for each tissue type (normal or cancer) was normalized separately (inverse normal transformation across samples and genes) before being used for the downstream analyses. We mapped the GTEx tissue types to the corresponding TCGA cancer types (Table S2b), resulting in one-on-many mappings, e.g. the normal lung tissue was mapped to both lung adenocarcinoma (LUAD) and lung squamous cell carcinoma (LUSC).

Cancer risk data and onset age

Lifetime cancer risk denotes the chance a person has of being diagnosed with cancer during his or her lifetime. Lifetime cancer risk data (Table S2a) are from Tomasetti and Vogelstein, 2015 (2), which are based on the US statistics from the SEER database (1). We derived the cancer onset age based on the age-specific cancer incidence data from the SEER database with the standard formula (32). Specifically, for each cancer type, SEER provides the incidence rates for 5-year age intervals from birth to 85+ years old. The cumulative incidence (CI) for a specific age range S is computed from the corresponding age-specific incidence rates (IR_i, $i \in S$) as $CI = 5\sum_{i \in S} IR_i$, and the corresponding risk is computed as $risk = 1 - \exp(-CI)$. The onset age for each cancer type (Table S3) was computed as the age when the CI from birth is 50% of the lifetime CI (i.e. birth to 85+ years old). Usually, the onset age defined as such is between two ages where the actual CI data is available, so the exact onset age was obtained by linear interpolation. Alternative parameters were used to define onset age (Supp. Note) in order to show the robustness of the correlation between tissue cSL load and cancer onset age based on different definitions.

Computing proliferation index (PI)

PI was computed for each sample from gene expression using a proliferation signature named meta-PCNA (24). PI was computed as the median expression values of the set of meta-PCNA genes defined in Venet *et al.* 2011 (24), and is regarded as a proxy for the rate of cell proliferation within a sample.

Computing cSL load

For each sample, we computed the number of cancer-derived SL gene pairs that have both genes lowly expressed, and divided it by the total number of cSLs available to get the cSL load per sample. In the ISLE method described by (20), low expression was defined as having expression levels below the 33 percentile in each tissue. Thus the ISLE-derived cSL gene pairs were shown to exhibit synthetic sickness effect when both genes in the gene pair are expressed at levels below the 33 percentile in each tissue, even though this appears to be a very tolerant cutoff (20). We therefore adopted the same criterion for low expression for the main results, although we also explored other low expression cutoffs to demonstrate the robustness of the results (Supp. Note).

Analyzing cSL load change through pre-cancer stages

A dataset of gene expression in normal tissue, 6 different stages of pre-cancer lesions, and squamous cell carcinoma in the lung was obtained from Mascaux *et al.*, 2019 (26), containing 122 samples in total. cSL load of each sample was computed as above. Box plots of cSL load against the different stages show a trend of cSL load decreasing from normal through earlier to later pre-cancer stages, as described in the main text. This overall trend was tested statistically with an ordinal logistic regression, where the ordered logit corresponding to the different stages were modelled from cSL load. The resulting coefficient of cSL load is negative (with statistical significance), meaning that a lower cSL load is associated with higher probability of a later stage through the cancer development.

Computing tissue cSL load and correlation with lifetime cancer risk

Tissue cSL load (TCL) of each tissue type is the median value of the cSL loads of all the samples (or a subpopulation of samples) in that tissue, with cSL load of a sample computed as above. For example, TCL for the older population (age ≥ 50 years) is the median cSL load for the samples of age ≥ 50 years in each tissue type. For analyzing the correlation between the TCLs computed from GTEx normal tissues and cancer risk, we

mapped the GTEx tissue types to the corresponding cancer types for which lifetime risk data are available from Tomasetti and Vogelstein, 2015 (2), resulting in 16 GTEx types mapped to 27 cancer types (Table S2a). Gallbladder non papillary adenocarcinoma, and Osteosarcoma of arms, head, legs and pelvis are not mapped to GTEx tissues and excluded from our analysis.

Computing cSL single-gene load

To investigate the effect on the single gene level, we computed the cSL single-gene load in a paralleling way to the computation of the cSL load. Among all the unique genes constituting the cSL network (i.e. cSL genes), we computed the fraction of lowly expressed cSL genes for each sample as the cSL single-gene load, where low expression was defined in the same way as the computation of cSL load as elaborated above. Similarly, tissue cSL single-gene load is the median value of the cSL single-gene loads of all the samples in a tissue.

Predicting tissue lifetime cancer risk with linear models

The lifetime cancer risks across tissue types were predicted with linear models containing three different sets of explanatory variables: (i) the number of total stem cell divisions (NSCD) alone, (ii) tissue cSL load alone, and (iii) NSCD together with tissue cSL load. Log-likelihood ratio (LLR) test was used to determine whether model (iii) (the full model) is significantly better than model (i) (the null model) in predicting lifetime cancer risks. The three models were also used to predict the lifetime cancer risks with a leave-one-out cross-validation procedure, and the prediction performances were measured by Spearman correlation coefficient. A similar analysis was performed to predict lifetime cancer risks across tissue types with three linear models involving the level of abnormal DNA methylation levels of the tissues (6): (i) the number of levels of abnormal DNA methylation (LADM) alone, (ii) tissue cSL load alone, and (iii) LADM together with tissue cSL load.

Identifying and analyzing released and retained cSLs

For each pair of GTEx normal-TCGA cancer of the same tissue type (Table S2b), we computed the fraction of samples where a cSL gene pair *i* has both genes lowly

expressed (defined above) among the normal samples (fn_i) and cancer samples (fc_i), and computed a *release score* as $rs_i = fn_i - fc_i$. We selected the released cSLs as those whose release scores are greater than the 75% percentile of all scores, and retained cSLs as those with a score below the 25% percentile (Table S4a,b). We compared SL significance scores between the released cSLs and retained cSLs in each tissue using a Wilcoxon rank-sum test. For each type of the GTEx normal tissues used in this analysis (i.e. those that can be mapped to TCGA cancer types), we also computed the tissue cSL load as above but using the released, retained, or all cSLs, respectively, and analyzed their correlation with lifetime cancer risk or cancer onset age across the tissues.

Pathway enrichment of the released cSLs

We designed an empirical enrichment test as below to account for the fact that each cSL consists of two genes. For the released cSLs in each tissue type and each given pathway from the Reactome database (33), we computed the odds ratio (OR) for the overlap between the genes in released cSLs and the genes within the pathway based on the Fisher's exact test procedure, with the "background" being all the genes in the ISLE-inferred cSLs. A greater than 1 OR indicates that the released cSLs are positively enriched for the genes of the pathway. To determine the significance of the enrichment, we repeatedly and randomly sampled the same number of cSLs as that of the released cSLs, computed the ORs similarly, and computed the empirical P value as the fraction of cases where the OR from the random cSLs is greater than that from the released cSLs. We corrected for multiple testing across pathways with the Benjamini-Hochberg method.

Analyzing the tissue-specificity of tumor suppressor genes

We obtained the list of TSGs and their associated tissue types from the COSMIC database (11) (https://cancer.sanger.ac.uk/cosmic/download, the "Cancer Gene Census" data. Table S6a). For each TSG, their cSL partner genes were identified using the ISLE pipeline (20) with an FDR cutoff of 0.1 (Table S6b). Here the FDR cutoff is more stringent than that used for the pan-cancer genome-wide cSL network (FDR < 0.2 for the main results) since here FDR correction was performed for each TSG, corresponding to a much lower number of multiple hypotheses. As a result, the FDR correction has more power and a relatively more stringent cutoff can give rise to a more reasonable number of cSL

partner genes per TSG. We focused our analysis on 23 TSGs for which more than one cSL partner genes were identified (no cSL partner was identified for most of the other TSGs). The expression levels of the cSL partner genes were then compared between tissue type(s) where the TSG is a known driver and the rest of the tissues where the TSG is not an established driver with linear models. Specifically, the expression levels of the cSL partners were modeled with two explanatory variables: (i) driver status of the TSG in the tissue (binary) and (ii) cSL partner gene (categorical, indicating each of the cSL partner genes of a TSG). The coefficient and P value associated with variable (i) were used to analyze the general trend of differential expression among the cSL partner genes. Positive coefficients of variable (i) means that the expression levels of the cSL partner genes are on average higher in the tissue(s) where the TSG is a known driver compared to those in the tissues where the TSG is not an established cancer driver.

Data/Code availability

The R code and the relevant data are available at https://hpc.nih.gov/~chengk6/SL_cancer_risk.zip.

Acknowledgments

This research was supported in part by the Intramural Research Program of the National Institutes of Health (NIH), National Cancer Institute and the Center for Cancer Research. This work utilized the computational resources of the NIH HPC Biowulf cluster (http://hpc.nih.gov). The Genotype-Tissue Expression (GTEx) Project was supported by the Common Fund of the Office of the Director of the National Institutes of Health, and by NCI, NHGRI, NHLBI, NIDA, NIMH, and NINDS. We thank Dr. Stephen J. Chanock, Dr. Brid M. Ryan, Dr. Tom Misteli, Prof. Sridhar Hannenhalli, Dr. Xin Wei Wang, Dr. Curtis C. Harris, Dr. Alejandro Schaffer, Dr. Michael Gertz, Dr. Kun Wang, Sushant Patkar, Sanju Sinha, and Dr. Fiorella Schischlik for their critical comments and suggestions on our study and the manuscript. K.C. is supported by the NCI-UMD Partnership for Integrative Cancer Research fellowship.

Author contributions

KC, NUN, ER formulated the research question and study design. KC, NUN carried out the analysis. JSL provided help with the computational cSL prediction pipeline. KC, NUN, ER analyzed the results. KC, NUN, ER wrote the manuscript with inputs from JSL. ER supervised the research. The manuscript has been read and approved by all the authors.

Author Information

Eytan Ruppin is a co-founder and scientific consultant of Pangea Therapeutics (https://pangeamedicine.com/) which focuses on precision oncology and synthetic lethality; however he has divested all his shares and receives no salary or financial benefit from this company. The work in this manuscript is not related to the work of this company. The other authors declare no conflict of interest. Correspondence and requests for materials should be addressed to <eytan.ruppin@nih.gov>.

References

1. SEER. Surveillance, Epidemiology, and End Results (SEER) Program (www. seer. cancer. gov) SEER*Stat Database Incidence - SEER 9 RegsResearch Data, Nov 2017 Sub (1973-2015) - Linked To County Attributes - Total U.S., 1969-2016 Counties, National Cancer Institute, DCCPS, Surveillance Research Program, released April 2018, based on the November 2017 submission. 2018.

2. Tomasetti C, Vogelstein B. Variation in cancer risk among tissues can be explained by the number of stem cell divisions. Science. 2015;347:78–81.

3. Tomasetti C, Li L, Vogelstein B. Stem cell divisions, somatic mutations, cancer etiology, and cancer prevention. Science. 2017;355:1330–4.

4. Wu S, Powers S, Zhu W, Hannun YA. Substantial contribution of extrinsic risk factors to cancer development. Nature. 2015;529:43–7.

5. Feinberg AP, Ohlsson R, Henikoff S. The epigenetic progenitor origin of human cancer. Nat Rev Genet. 2006;7:21–33.

6. Klutstein M, Moss J, Kaplan T, Cedar H. Contribution of epigenetic mechanisms to variation in cancer risk among tissues. Proc Natl Acad Sci. 2017;114:2230–4.

7. Sauer AG, Siegel RL, Jemal A, Fedewa SA. Current Prevalence of Major Cancer Risk Factors and Screening Test Use in the United States: Disparities by Education and Race/Ethnicity. Cancer Epidemiol Prev Biomark. 2019;28:629–42.

8. Armitage P, Doll R. The age distribution of cancer and a multi-stage theory of carcinogenosis. Int J Epidemiol. 2004;33:1174–9.

9. Bailey MH, Tokheim C, Porta-Pardo E, Sengupta S, Bertrand D, Weerasinghe A, et al. Comprehensive Characterization of Cancer Driver Genes and Mutations. Cell. 2018;173:371-385.e18.

10. Haigis KM, Cichowski K, Elledge SJ. Tissue-specificity in cancer: The rule, not the exception. Science. 2019;363:1150–1.

11. Tate JG, Bamford S, Jubb HC, Sondka Z, Beare DM, Bindal N, et al. COSMIC: the Catalogue Of Somatic Mutations In Cancer. Nucleic Acids Res. 2019;47:D941–7.

12. Elledge SJ, Amon A. The BRCA1 suppressor hypothesis: an explanation for the tissue-specific tumor development in BRCA1 patients. Cancer Cell. 2002;1:129–32.

13. Schneider G, Schmidt-Supprian M, Rad R, Saur D. Tissue-specific tumorigenesis: context matters. Nat Rev Cancer. 2017;17:239–53.

14. Bridges CB. The origin of variations in sexual and sex-limited characters. Amer Nat. 1922;56:51–63.

15. Bender A, Pringle JR. Use of a screen for synthetic lethal and multicopy suppressee mutants to identify two new genes involved in morphogenesis in Saccharomyces cerevisiae. Mol Cell Biol. 1991;11:1295–305.

16. Hartwell LH, Szankasi P, Roberts CJ, Murray AW, Friend SH. Integrating genetic approaches into the discovery of anticancer drugs. Science. 1997;278:1064–8.

17. Lord CJ, Ashworth A. PARP inhibitors: Synthetic lethality in the clinic. Science. 2017;355:1152–8.

18. O'Neil NJ, Bailey ML, Hieter P. Synthetic lethality and cancer. Nat Rev Genet. 2017;18:613–23.

19. Parameswaran S, Kundapur D, Vizeacoumar FS, Freywald A, Uppalapati M, Vizeacoumar FJ. A Road Map to Personalizing Targeted Cancer Therapies Using Synthetic Lethality. Trends Cancer. 2019;5:11–29.

20. Lee JS, Das A, Jerby-Arnon L, Arafeh R, Auslander N, Davidson M, et al. Harnessing synthetic lethality to predict the response to cancer treatment. Nat Commun. 2018;9:2546.

21. Feng X, Arang N, Rigiracciolo DC, Lee JS, Yeerna H, Wang Z, et al. A Platform of Synthetic Lethal Gene Interaction Networks Reveals that the GNAQ Uveal Melanoma Oncogene Controls the Hippo Pathway through FAK. Cancer Cell. 2019;35:457-472.e5.

22. The Cancer Genome Atlas Research Network, Weinstein JN, Collisson EA, Mills GB, Shaw KRM, Ozenberger BA, et al. The Cancer Genome Atlas Pan-Cancer analysis project. Nat Genet. 2013;45:1113–20.

23. GTEx Consortium. The Genotype-Tissue Expression (GTEx) project. Nat Genet. 2013;45:580–5.

24. Venet D, Dumont JE, Detours V. Most Random Gene Expression Signatures Are Significantly Associated with Breast Cancer Outcome. PLOS Comput Biol. 2011;7:e1002240.

25. Marcotte R, Sayad A, Brown KR, Sanchez-Garcia F, Reimand J, Haider M, et al. Functional Genomic Landscape of Human Breast Cancer Drivers, Vulnerabilities, and Resistance. Cell. 2016;164:293–309.

26. Mascaux C, Angelova M, Vasaturo A, Beane J, Hijazi K, Anthoine G, et al. Immune evasion before tumour invasion in early lung squamous carcinogenesis. Nature. 2019;571:570–5.

27. Magen A, Das Sahu A, Lee JS, Sharmin M, Lugo A, Gutkind JS, et al. Beyond Synthetic Lethality: Charting the Landscape of Pairwise Gene Expression States Associated with Survival in Cancer. Cell Rep. 2019;28:938-948.e6.

28. Mullard A. Synthetic lethality screens point the way to new cancer drug targets. Nat Rev Drug Discov. 2017;16:736.

29. Horlbeck MA, Xu A, Wang M, Bennett NK, Park CY, Bogdanoff D, et al. Mapping the Genetic Landscape of Human Cells. Cell [Internet]. 2018 [cited 2018 Aug 3];0. Available from: https://www.cell.com/cell/abstract/S0092-8674(18)30735-9

30. Mailman MD, Feolo M, Jin Y, Kimura M, Tryka K, Bagoutdinov R, et al. The NCBI dbGaP database of genotypes and phenotypes. Nat Genet. 2007;39:1181–6.

31. Goldman M, Craft B, Hastie M, Repečka K, McDade F, Kamath A, et al. The UCSC Xena platform for public and private cancer genomics data visualization and interpretation. bioRxiv. 2019;326470.

32. Parkin DM, Muir CS, Whelan SJ, Gao YT, Ferlay J, Powell J. Cancer Incidence in Five Continents. Lyon: IARC; 1992.

33. Fabregat A, Jupe S, Matthews L, Sidiropoulos K, Gillespie M, Garapati P, et al. The Reactome Pathway Knowledgebase. Nucleic Acids Res. 2018;46:D649–55.